Rotational Fourier tracking of diffusing polygons

Kenny Mayoral,[1] Terry P. Kennair,[1] Xiaoming Zhu,[1] James Milazzo,[2,*] Kathy Ngo,[1]
Michael M. Fryd,[1] and Thomas G. Mason[1,2,3,†]

[1]*Department of Chemistry and Biochemistry, University of California, Los Angeles, Los Angeles, California 90095, USA*
[2]*Department of Physics and Astronomy, University of California, Los Angeles, Los Angeles, California 90095, USA*
[3]*California NanoSystems Institute, University of California, Los Angeles, Los Angeles, California 90095, USA*

We use optical microscopy to measure the rotational Brownian motion of polygonal platelets that are dispersed in a liquid and confined by depletion attractions near a wall. The depletion attraction inhibits out-of-plane translational and rotational Brownian fluctuations, thereby facilitating in-plane imaging and video analysis. By taking fast Fourier transforms (FFTs) of the images and analyzing the angular position of rays in the FFTs, we determine an isolated particle's rotational trajectory, independent of its position. The measured in-plane rotational diffusion coefficients are significantly smaller than estimates for the bulk; this difference is likely due to the close proximity of the particles to the wall arising from the depletion attraction.

I. INTRODUCTION

The common availability of optical microscopes and digital video hardware in many research laboratories has led to the widespread use of video particle tracking microscopy (VPTM). Movies that capture many kinds of interesting and complex transport phenomena, including instabilities of driven fluids in microfluidic devices [1,2], Brownian diffusion of microscopic probe particles in viscoelastic media [3], and time-lapse dynamics of the division of biological cells [4], have been recorded. Although movies containing such interesting microscopic phenomena can be readily made, performing quantitative image analysis to measure relevant transport properties can frequently be challenging. Thus opportunities yet remain for improving the experimental measurement of microscopic phenomena captured by VPTM.

In particular, the rotational mobilities of nonspherical probe particles, even in a simple viscous liquid, have not been accurately measured or predicted for many different kinds of shapes having reduced symmetry. Although the translational and rotational Stokes drag, and therefore diffusion coefficients, have been calculated for circular platelets (i.e., disks) in a bulk fluid at low Reynolds number [5–7], calculations of the Stokes drag for more complex shapes, such as polygonal platelets, have not been made. Since a variety of lithographic methods now enable production of microscale and nanoscale complex platelets [8–10], even with such intricate geometries as the alphabet [9], it is now possible to experimentally observe and record the diffusion coefficients of platelets having a wide variety of shapes in two dimensions using optical microscopy.

While significant attention has been given to determining the center positions of spherical colloidal probe particles through VPTM [11–13] and more complicated laser deflection [14] and interferometry methods [15], much less attention has been given to rotational tracking. Light streak tracking, which involves detecting focused laser light scattered from a single microparticle, has achieved good accuracy in determining mean-square angular displacements (MSADs) of disks [16]; this method has been used to perform passive rotational microrheology of polymeric solutions [17]. Although a video particle tracking routine that determines the center positions and vertices of polygons at high densities has been developed and used [18,19], this simple single-vertex identification approach has somewhat limited precision. Thus it would be desirable to develop a robust image analysis technique that more fully utilizes the angular information in digital images and could therefore more accurately determine the angular trajectories of a variety of custom-shaped probe particles.

Here we introduce a versatile Fourier method for analyzing video movies that can precisely determine the angular orientation of an isolated colloidal particle that, when imaged, has a nontrivial cross-sectional projection. To demonstrate this method, we use optical VPTM to measure the rotational diffusion of triangular and square-shaped lithographic polygonal platelets confined in two dimensions near a solid wall by a depletion attraction. Using the Fourier approach, we obtain angular trajectories, MSADs, and the rotational diffusion coefficients without having to locate the center positions of the particles. Because this Fourier image analysis method does not inherently depend on the type of microscopy used, in principle, it could be applied to images or movies made using other forms of microscopy, such as electron microscopy, x-ray microscopy, or even time-resolved surface probe microscopy (e.g., atomic force microscopy).

II. EXPERIMENT

Platelike microscale lithographic particles (e.g., equilateral triangular and square prisms) composed of an epoxy photoresist polymer SU-8 are prepared using an Ultratech i-line XLS stepper, according to a protocol established previously for mass-producing exotic-shaped colloids [9]. This top-down production process produces about 10^8 microplatelets per 5 inch diameter wafer; these particles are then lifted off of the wafer and dispersed in an aqueous surfactant solution (1-mM sodium dodecyl sulfate) that stabilizes the released particles against aggregation.

---

*Present address: Department of Physics, New York University, 4 Washington Place, New York, New York 10003, USA.

†Corresponding author: mason@physics.ucla.edu

In order to prevent thermally induced tipping and elevation of platelets above the flat surface of the confining cuvette's glass wall, we restrict their diffusion to two dimensions utilizing roughness-controlled depletion attractions. These are generated by adding depletion agents of anionically stabilized polystyrene spheres that keep the faces of particles near the surface of a glass coverslip [20]. The concentration and size of the depletion agent, as well as the area contributing to the excluded volume of the microscale particle, all strongly affect the strength of the depletion attraction. Therefore, this concentration is adjusted to provide a similar strength of attraction for different surface areas of the flat faces of the platelets [20]. In particular, a highly dilute aqueous dispersion of regular triangular particles (platelet volume fraction $\phi \approx 10^{-5}$), having an edge length of 2.7 μm and a thickness of 1.0 μm, is added to an aqueous dispersion of polystyrene spheres (20 nm in diameter), yielding a final volume fraction $\phi_s = 0.5\%$ for the depletion agent. As fabricated, square platelets have an edge length of 4.5 μm and a thickness of 1.0 μm, so a somewhat smaller volume fraction $\phi_s = 0.1\%$ of the same depletion agent can be used in order to achieve a similar degree of two-dimensional confinement. Separately, these colloidal mixtures containing either triangles or squares are loaded into a rectangular glass microcuvette, sealed to inhibit convection, and imaged using optical microscopy (Nikon TE2000 inverted microscope, brightfield, 100× objective, 1.40 numerical aperture, PointGrey Flea2 CCD 1024 × 768 pixels, 30 frames per second) after the particles have sedimented and been restricted by depletion attractions to diffuse in-plane just above the lower wall of the cuvette. To simplify the experimental imaging and inhibit undesired particle aggregation, we restrict our attention to a highly dilute dispersion of platelets so that only a single particle is typically observed in a field of view. All measurements have been made at room temperature $T = 297 \pm 1$ K.

III. ANALYSIS

An example of an acquired image of the triangular platelet is shown in Fig. 1(a). Edge detection is used to create a sharp high-contrast 8-bit grayscale image of the particle, as shown in Fig. 1(b) [12]. This high-contrast image is fast Fourier transformed to the Fourier domain. Because the particle's edges are straight and well defined over many pixels, the resulting (log-scaled, amplitude-squared) transform exhibits a set of rays, as shown in Fig. 1(c); each ray is perpendicular to a corresponding edge of the particle [21]. For each frame of the resulting preprocessed fast Fourier transform (FFT) video, an automated program (LabView) detects the locations of each intensity peak as a function of azimuthal angle θ in the FFT at a particular radius around the center of the image. To obtain sharp intensity peaks exhibiting a high signal-to-noise ratio, we set the radius in reciprocal space to be 70 pixels for triangles and 50 pixels for squares; the ring's effective width is 1 pixel [e.g., see the white ring in Fig. 1(c)]. A parabolic fitting algorithm is used to detect the centers of the peaks (six for triangles), shown as the vertical dashed lines in Fig. 1(d). By comparing this set of peak locations with the ideal case of peaks separated by $\pi/3$ for equilateral triangles, we obtain an average orientation angle θ, modulo 2π. By tracking a particular peak from frame to frame, the routine corrects for abrupt jumps in
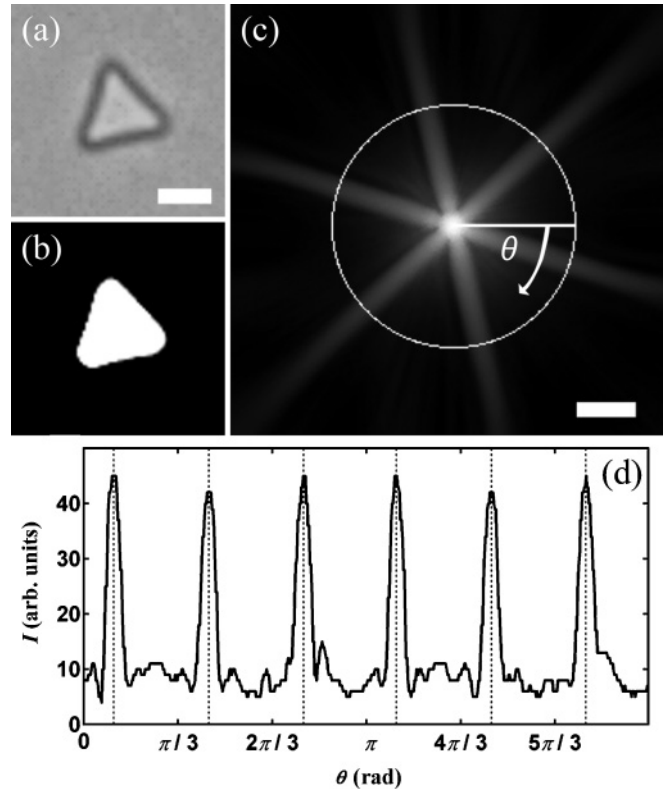

FIG. 1. Fourier transform analysis yields the angular orientation of an isolated triangular polygon without requiring any identification of its position. The (a) real-space image obtained from optical video microscopy is transformed to (b) a grayscale (appearing nearly binary) image using edge detection and a Fourier transform intensity of the grayscale image generates (c) a spokelike FFT having six rays with angles that reflect the triangle's orientation. The intensity of these rays is measured azimuthally along a set radius [the white ring in (c) has a radius of 70 pixels], yielding (d) $I(\theta)$ having six peaks. Peak detection identifies the maxima in $I(\theta)$ (vertical dashed lines) and these angles are used to more accurately determine the absolute orientation of the triangle associated with one vertex. The real-space scale bar in (a) is 3 μm; the reciprocal space scale bar in (c) is 4 μm^{-1}.

any peak locations due to the 2π periodicity, thus providing the absolute change in angle θ over long periods of time t. For square particles, four rather than six rays are seen in the FFTs, corresponding to the reduced number of edges, as shown in Fig. 2. The rotational tracking process produces absolute angular positions with a resolution of 20 mrad based upon the averaging of the detected peaks in each frame. In our digital videos, triangles have an approximate edge length of 29 pixels and the squares have an edge length of 37 pixels, so an edge length of about 30 pixels can provide about 20-mrad resolution. Whether for triangles or squares, after obtaining the angular trajectory, the MSAD $\langle \Delta\theta^2(t) \rangle$ is calculated and the particle's in-plane rotational diffusion coefficient D_r is determined from the slope of a linear least-squares fit of $\langle \Delta\theta^2(t) \rangle = 2D_r t$ in the short-time limit.

IV. RESULTS AND DISCUSSION

A representative angular trajectory $\theta(t)$ of a triangular particle is shown in the bottom right inset of Fig. 3. This trajectory
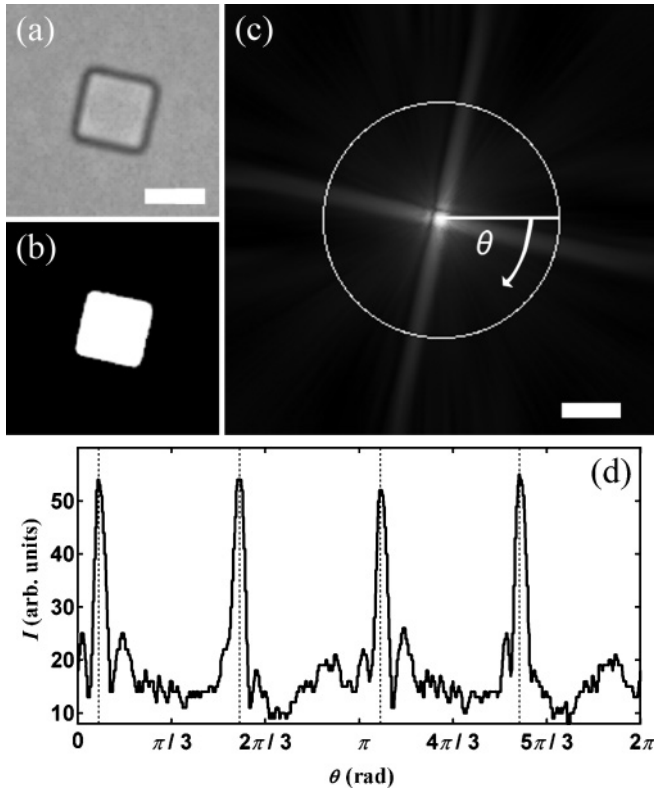
FIG. 2. Fourier transform analysis of a square particle, paralleling the results shown in Fig. 1: (a) optical micrograph, (b) grayscale image after edge detection, (c) FFT showing four rays corresponding to the two sets of parallel edges of the square (the white ring has a radius of 50 pixels), and (d) intensity as a function of angle $I(\theta)$ shown with peak-detected angles (vertical dashed lines). The real-space scale bar in (a) is 4 μm; the reciprocal space scale bar in (c) is 1 μm^{-1}.
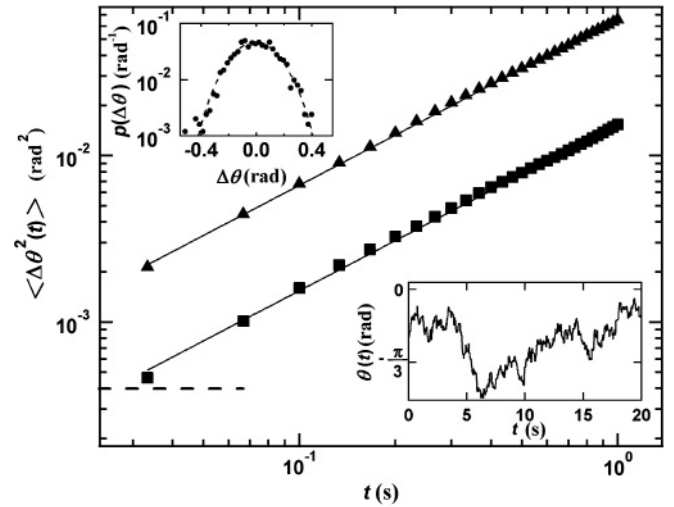

FIG. 3. Calculated mean-square angular displacement $\langle \Delta\theta^2(t) \rangle$ versus time t for square platelets (solid squares) and triangular platelets (solid triangles). Solid lines are linear least-squares fits of $\langle \Delta\theta^2(t) \rangle = 2D_r t$, where D_r is the in-plane rotational diffusion coefficient, yielding $D_r = 3.3 \pm 0.2 \times 10^{-2}$ rad^2/s (triangles) and $D_r = 8.3 \pm 0.5 \times 10^{-3}$ rad^2/s (squares). The horizontal dashed line represents the lower bound of the angular resolution determined for triangles (0.020 rad). The top left inset shows the measured angular step-size distribution $p(\Delta\theta)$ from a trajectory set with 1800 frames for a diffusing triangle, corresponding to a fixed time interval between frames of 0.033 s (the dashed line is a fit to a Gaussian distribution). The bottom right inset shows a portion of the rotational trajectory $\theta(t)$ of a triangular platelet determined using the Fourier analysis technique in Fig. 1.

has the expected characteristics of a one-dimensional random walk. The top left inset of Fig. 3 shows a sample probability distribution for an angular step between consecutive frames $p(\Delta\theta)$; the distribution is Gaussian (the dashed line is a fit), as expected for rotation driven by Brownian motion. Since the angular resolution is high enough, the calculated MSADs for both triangles and squares are linear down to the earliest times measured, as shown in Fig. 3. The angular Brownian motion of the platelet particles near the solid wall yields rotational diffusion coefficients of $D_r = 3.3 \pm 0.2 \times 10^{-2}$ rad^2/s for triangles and $D_r = 8.3 \pm 0.5 \times 10^{-3}$ rad^2/s for squares. The smaller diffusion coefficient of a square is consistent with its larger edge length (i.e., greater maximal spatial dimension) compared to triangles.

It would be interesting to compare these results with a relevant theory that could account for the rotational diffusion of triangular and square platelet particles in close proximity to a wall in the presence of strong depletion interactions; unfortunately, no theory that incorporates this complexity has yet been developed. Consequently, we simply compare the measured diffusion coefficients with the closest available theory, a calculation in the bulk for thin disks having similar lateral dimensions. The rotational diffusion coefficient for a thin disk having radius a diffusing in a bulk fluid having a viscosity η can be estimated in the low-frequency, low-Reynolds-number limit as $D_r = 3k_BT/(32\eta a^3)$ [6]. Using the circumscribed radius of the triangle for a, its rotational diffusion coefficient is estimated to be 3.8×10^{-1} rad^2/s. Our measured rotational diffusion coefficient for a triangle is about an order of magnitude smaller than this estimate, likely due to a combination of effects that arise from additional drag from the nearby solid wall and the presence of the depletion attraction, both of which can reduce the rate of rotational diffusion of the polygon. Although we have not directly measured the thickness of the lubricating layer of water between the platelets and the solid wall, we estimate it to be ≈ 50 nm, somewhat larger than the average roughness height on the faces of the particles, which is comparable to the size of the depletion agent.

Confining platelet particles to two dimensions using a depletion agent is one convenient way to facilitate video imaging; other realizations of experiments that provide a time sequence of images of an isolated rotating particle, whether driven diffusively or convectively, could also be used. Indeed, images showing the reorientation of complex particles that have at least one straight edge should be able to take advantage of the Fourier ray-tracking algorithm, even if only two primary rays in the FFT are generated from the straight edge. In principle, the Fourier analysis method we have demonstrated for isolated particles can be extended to several particles in the same field of view. However, interpreting the resulting superposition of rays from different particles may become ill-posed if certain rays overlap and cannot be uniquely distinguished in the FFT

intensity (e.g., if two or more particles having the same shapes are in the field of view). Each additional particle in the field of view will add another set of rays to the FFT. Nevertheless, by using phase information of the FFT, it may be possible to extend the technique we have presented to track the rotations of multiple particles, for which the contributions to the FFT intensity of specific rays originating from certain particles can be uniquely labeled using the FFT phase information. The FFT phase effectively encodes particle positions, and we have shown that considering the phase information is not necessary when determining the angular orientation of an isolated single particle.

While we have shown that the Fourier method provides a way to assess the orientation of a particle having a nontrivial cross-sectional projection in two dimensions, we anticipate that this method can be readily extended into three dimensions by taking the three-dimensional Fourier transforms of, for instance, individual volume frames of confocal microscopy movies of isolated facetted particles. The Fourier transform would result in a set of rays (i.e., spokes) in three-dimensional reciprocal space emanating in directions normal to the facets of the particle, analogous to the rays we have shown in two dimensions for polygons. Tracking the spokes would require adapting the current algorithm into three dimensions using an approach analogous to the method we have presented here.

Although the rotational diffusion of particles and molecules has been measured in many other cases, these results cannot be directly compared with the results of our experiments due to significant differences in the shapes and sizes of the diffusing particles and also the differences in boundary conditions (i.e., proximity to a wall). A system of rotating prolate ellipsoids, for example, has been made using a thin glass cell having a thickness of about one micron (over a localized area) as the method of confinement [22]. In this case the ellipsoids are near two solids walls, whereas in our experiments the depletion attraction keeps the polygonal platelets near only one solid wall. Although measurements of diffusion coefficients for translating and rotating rods near a surface have been made [23], the friction coefficients for these objects (i.e., shape and aspect ratio) are not similar to the polygons we have examined. More work, whether simulations or theory, on anisotropic, complex-shaped particles is needed to fully understand the complicated hydrodynamics of particles undergoing rotational and translational diffusion in the bulk and near walls. A suitable theory that could potentially address our measurements would consider the in-plane rotational Stokes drag of regular polygonal platelets confined near a solid wall by a depletion attraction, separated by only a very thin layer of lubricating viscous liquid, yielding the in-plane rotational mobility and diffusion coefficient. Such a calculation would enable a direct quantitative comparison with our experimental results and would be beneficial in advancing the understanding of the diffusion of anisotropic, complex-shaped particles.

We have shown that Fourier analysis of optical micrographs of isolated polygonal platelets can be used for rotational tracking, independent of particle position. Although we have presented detailed results for only two types of regular polygons, triangles and squares, this approach may be extended to many kinds of platelets. Among the easiest to track, platelets having well-defined linear edges are especially well suited, provided the number of edges is not so large that the rays in the FFT intensity overlap and cannot therefore be distinguished by peak detection. Furthermore, this technique can be applied in a straightforward manner for less symmetric shapes, other than regular polygons, provided there is at least one well-defined straight edge on the particle that will give rise to a bright line of intensity in the FFT. Indeed, the technique could be extended to particle shapes having complex curved edges using pattern recognition of a complex continuous set of rays in Fourier space (i.e., by performing a correlation analysis of the Fourier pattern of an initial frame of the FFT movie with an angularly rotated version of a Fourier pattern in subsequent frames). Increasing the particle's size in pixels in images and also the frame acquisition rate of the camera could provide a means of sensitively probing rotational diffusion useful in microrheology applications of thin layers of materials between the platelet and solid wall over a wide dynamic range.

V. CONCLUSION

The rotational Brownian motion of complex-shaped particles can be accurately measured by Fourier transform analysis. By tracking peaks in $I(\theta)$, one can extract rotational diffusion coefficients for many different complex particle shapes, as we have demonstrated with equilateral triangles and squares. Not surprisingly, the values of the rotational diffusion coefficients of these platelike particles confined near a solid wall by a depletion attraction are substantially lower than an estimate of rotational diffusion coefficients of a thin circumscribed disk diffusing in the bulk. This points out the need for translational and rotational Stokes drag calculations of complex shapes in the bulk and near a wall in the presence of a depletion agent. In the future, the Fourier analysis technique can potentially facilitate translational tracking of the particle in a subsequent analysis, since its orientation has been predetermined. Moreover, this analysis approach for isolated particles may also be extended to several particles in a field of view if the phase information of the FFT is appropriately considered.

[1] T. Cubaud and T. G. Mason, Phys. Rev. Lett. **96**, 114501 (2006).

[2] T. M. Squires and J. F. Brady, Phys. Fluids **17**, 073101 (2005).

[3] T. M. Squires and T. G. Mason, Annu. Rev. Fluid Mech. **42**, 413 (2010).

[4] C. Papan, B. Boulat, S. S. Velan, S. E. Fraser, and R. E. Jacobs, Dev. Dyn. **235**, 3059 (2006).

[5] H. Brenner, J. Fluid Mech. **18**, 144 (1964).

[6] W. Zhang and H. A. Stone, J. Fluid Mech. **367**, 329 (1998).

[7] H. Lamb, *Hydrodynamics* (Cambridge University Press, London, 1932).

[8] M. D. Hoover, S. A. Casalnuovo, P. J. Lipowicz, H. C. Yeh, R. W. Hanson, and A. J. Hurd, J. Aerosol Sci. **21**, 569 (1990).

[9] C. J. Hernandez and T. G. Mason, J. Phys. Chem. C **111**, 4477 (2007).

[10] M. Sullivan, K. Zhao, C. Harrison, R. H. Austin, M. Megens, A. Hollingsworth, W. B. Russel, Z. Cheng, T. G. Mason, and P. M. Chaikin, J. Phys.: Condens. Matter **15**, S11 (2003).

[11] T. G. Mason, A. Dhople, and D. Wirtz, in *Statistical Mechanics in Physics and Biology*, edited by D. Wirtz and T. C. Halsey, MRS Symposia Proceedings No. 463 (Materials Research Society, Pittsburgh, 1997), p. 153.

[12] J. C. Crocker and D. G. Grier, J. Colloid Interface Sci. **179**, 298 (1996).

[13] C. A. Murray and D. G. Grier, Annu. Rev. Phys. Chem. **47**, 421 (1996).

[14] T. G. Mason, K. Ganesan, J. H. van Zanten, D. Wirtz, and S. C. Kuo, Phys. Rev. Lett. **79**, 3282 (1997).

[15] F. Gittes, B. Schnurr, P. D. Olmsted, F. C. MacKintosh, and C. F. Schmidt, Phys. Rev. Lett. **79**, 3286 (1997).

[16] Z. Cheng, P. M. Chaikin, and T. G. Mason, Phys. Rev. Lett. **89**, 108303 (2002).

[17] Z. Cheng and T. G. Mason, Phys. Rev. Lett. **90**, 018304 (2003).

[18] K. Zhao, R. Bruinsma, and T. G. Mason, Proc. Natl. Acad. Sci. USA **108**, 2684 (2011).

[19] K. Zhao and T. G. Mason, Phys. Rev. Lett. **103**, 208302 (2009).

[20] K. Zhao and T. G. Mason, Phys. Rev. Lett. **99**, 268301 (2007).

[21] J. C. Russ, *The Image Processing Handbook* (CRC, Boca Raton, FL, 1992).

[22] Y. Han, A. M. Alsayed, M. Nobili, J. Zhang, T. C. Lubensky, and A. G. Yodh, Science **314**, 626 (2006).

[23] J. T. Padding and W. J. Briels, J. Chem. Phys. **132**, 054511 (2010).